Chemistry–A European Journal
Research Article
doi.org/10.1002/chem.202401944
Chemistry Europe
European Chemical Societies Publishing
www.chemeurj.org

Fast and Efficient Sensing of Drugs in Water Using Self-Assembling D-Glucamine-Functionalized Naphthalenediimide and 1,8-Naphthalimide Fluorophores

Salvatore Marullo,*[a] Riccardo Arena,[a] Giuseppe Lazzara,[b] Giuseppe Cavallaro,[b] Michele Cacioppo,[a] and Francesca D'Anna*[a]

[a] this work.

Fast and sensitive quantification of drugs as emerging pollutants in water bodies is a pressing need in contemporary society, to prevent serious environmental concerns that could negatively impact on human health. This explains the surge of interest in this field, and the need to identify highly selective sensing systems. Addressing this issue, in this work we synthesized two D-glucamine functionalized fluorophores bearing self-assembling cores, as 1,8-naphthalimide and naphthalene diimide. We studied their self-assembly in water solution, and characterized the aggregated formed by determining their stability constant, their morphology and size by scanning electron microscopy, resonance light scattering and dynamic light scattering, as well their solid-state emission ability. Then, we studied their sensing ability, in water, towards pharmaceutically active compounds such as ciprofloxacin, nalidixic acid, carbamazepine and diclofenac sodium salt, by fluorescence investigation. Data collected show that the self-assembling ability is significantly affected by the fluorophore structure, which in turn also determines sensing ability. In particular, the naphtalene diimide-based probe was the most sensitive, with LOD as low as 0.01 μM in the presence of nalidixic acid, which is in line and competitive with more complex sensing systems, recently reported in the literature.

Introduction

Contrasting pollution of water bodies and environment is a pressing problem in present day society, and it involves the two-fold task of removing pollutants and also monitoring their presence. Recently, there has been an increasing concern about the presence in water bodies of chemicals known as emerging pollutants (EPs), which are defined as potentially harmful compounds, whose presence in water has not yet been regulated, or that are not part of routine analysis protocols.[1]

These molecules belong to a wide range of classes and structures, encompassing disinfectants, personal care products, plastic additives, plasticizers and pharmaceutically active compounds.[2]

These latter represent one of the most abundant categories of EPs, comprising especially non-steroidal anti-inflammatory drugs and antibiotics, deriving both from domestic sources or healthcare facilities.[3]

They have received increasing attention as they pose threats on environmental and human lives. Even at very low concentration, they can cause harm to living organisms and natural ecosystems as they are able to exert biological activity.[4,5] Their diffusion in the environment is a direct consequence of the growth in population, climate changes and increase in human activities.[6] Antibiotics can induce bacterial resistance,[7] while anti-inflammatory and psychiatric drugs, like diclofenac and carbamazepine, are able to induce oxidative stress not only on algae but also on mussels.[8]

Consequently, detection also at very low concentration of such compounds in water bodies is essential. Among the various methods available, a prominent role is played by fluorimetric sensing methods,[9] which can in principle combine high sensitivity and selectivity, low detection limit with fast, on-site response.[10]

In general, fluorescent chemosensors interact with the analytes by non-covalent forces, showing variation of their emission through a variety of possible mechanisms, including fluorescence turn-off or turn-on, aggregation induced emission or photoinduced electron transfer.[11]

Following this approach, different supramolecular interactions can be used to achieve sensitive detection of analytes, such as host-guest interaction between sensor and analyte, metal ion coordination or hydrogen bond-based molecular

[a] S. Marullo, R. Arena, M. Cacioppo, F. D'Anna
Dipartimento di Scienze e Tecnologie Biologiche, Chimiche e Farmaceutiche, Università degli Studi di Palermo, Viale delle Scienze, Ed. 17, 90128 Palermo, Italy
E-mail: salvatore.marullo@unipa.it
francesca.danna@unipa.it

[b] G. Lazzara, G. Cavallaro
Dipartimento di Fisica e Chimica, Università degli Studi di Palermo, Viale delle Scienze, Ed. 17, 90128 Palermo, Italy

Supporting information for this article is available on the WWW under https://doi.org/10.1002/chem.202401944

recognition.[12] To this purpose, host-guest interaction has been used to detect the presence in water bodies of pharmaceutically active compounds, using systems based on metal organic frameworks[13] or dansylated squaramide receptors.[14] On the other hand, a further attractive strategy is the one foreseeing the use of supramolecular aggregates as sensory systems.[15–18] In such cases, the sensor is constituted by supramolecular aggregates formed by a suitable fluorescent monomer, whose emission can change in the presence of a given analyte. The analyte can perturb the supramolecular aggregates both by inducing aggregation or disaggregation, thereby affecting the observed fluorescence emission. This approach has the advantage to employ often very simple molecules, and has been applied for the obtainment of ultrasensitive sensors, based on supramolecular aggregate of π -conjugated molecules such as perylene bisimide (PBI) or pyrene derivatives. For instance, simple PBI-functionalized ammonium salts have been successfully used as chiral sensors for α -hydroxycarboxylates,[19] while aggregates of pyrene-based pyridinium salts proved efficient and sensitive sensors for glucose.[20] Interestingly, aggregates of 3,4-diamine-naphthalimide derivatives have been successful used to detected thionyl and oxalyl chloride,[21] whereas a sensitive and selective fluorescent sensor for berberine chloride has been designed taking advantage from the emission behaviour of amino acid-functionalized PBI nucleus.[22]

Based on these considerations, we synthesized two fluorescent probes, bearing the 1,8-naphthalimide and the naphthalene diimide cores functionalized with D-glucamine, namely **NI-Glu** and **NDI-Glu**, depicted in Scheme 1.

We chose these molecules since their aromatic cores are well-known aggregating motifs, able to yield emissive aggregates in solution.[23,24] In addition, functionalization with D-glucamine moieties, should enhance solubility in water and hydrogen bonding abilities, increasing in principle the number of sites involved in aggregation and also interaction with analytes in solution. Indeed, there are several reports in the literature showing that D-glucamine,[25,26] or its methylated derivative,[27,28] can enhance water solubility of lipophilic self-assembling molecules, also affecting the aggregation propensity.

We studied the self-assembly of these compounds, in aqueous solutions, by concentration and temperature-dependent UV-vis and fluorescence investigations, and gathered information on the aggregates size and morphology by means of dynamic light scattering (DLS), resonance light scattering (RLS) and scanning electron microscopy (SEM). Then, we studied the possibility of using these aggregated systems as fluorescent sensors for the detection of pharmaceutically active compounds in aqueous solutions. To this aim, we chose drugs belonging to different classes, either neutral or charged as diclofenac sodium salt (DCF), carbamazepine (CBZ), ciprofloxacin (CP) and nalidixic acid (NA), reported in These drugs were chosen because they are among the category of largely consumed drugs, such as anti-convulsant, antibiotic and anti-inflammatory drugs. Moreover, they also differ significantly in structural characteristics like π-surface area extension, and presence of charged sites. In this respect, we considered an anionic drug, DCF, two compounds present in zwitterionic form in water, like CP and NA,[29,30] and a compound devoid of charged sites, like CBZ. We also carried out NMR and FTIR investigations to probe which interactions occur between the fluorophores and the drugs. Data collected shed light on the ability of fluorescent probes to give self-assembled systems with features highly dependent of the nuclei structure. These systems proved able to sense pharmaceutically active compounds at very low concentration. In particular, drug being the same, **NDI-Glu** was more sensitive than **NI-Glu**, as expressed by the limits of detection (LOD) and limit of quantification values (LOQ) which, being as low as $6{\cdot}10^{-8}$ M, in some cases proved competitive with more complex sensing systems, recently reported in the literature. Finally, we also conducted fluorescence measurements aimed at assessing the selectivity of the fluorophores in the presence of more than one drug in solution.

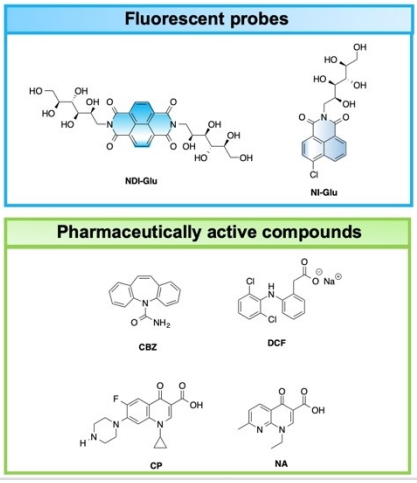

Scheme 1. Structures of fluorescent probes and pharmaceutically active compounds.

Results and Discussion

Synthesis of Fluorophores

Both salts were obtained in one step and good yields, by condensation of the relevant anhydride with D-glucamine, as reported in Scheme 2, following a modification of procedures reported in literature for the functionalization of similar nuclei.[31–33]

We chose to functionalize our fluorophores with D-glucamine with the aim to enhance solubility in water and their self-assembling ability, providing hydrogen bond donor groups. It is indeed well-known that the self-assembly of both nuclei often occurs by an interplay of π-stacking and hydrogen bonding.[34–36]

We then set out to investigate the self-assembling ability of our compounds. For the sake of clarity, we will describe the self-assembly ability investigation separately, for NDI-Glu and NI-Glu.

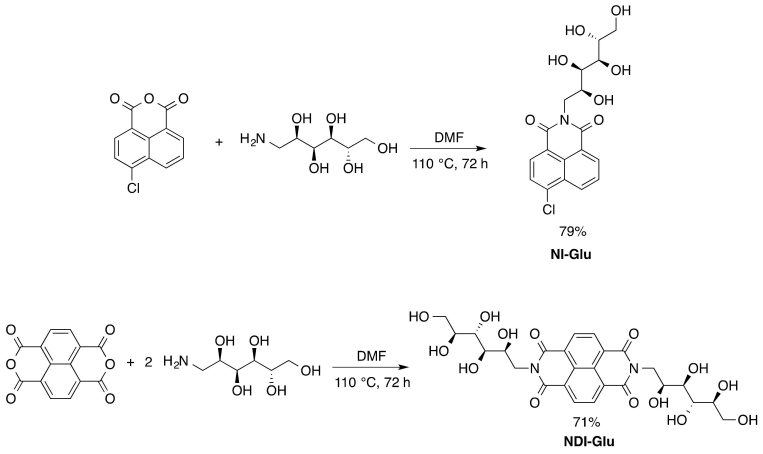

Scheme 2. Synthesis of fluorescent probes **NI-Glu** and **NDI-Glu**.

Self-Assembly of the Fluorophores. The Effect of Solvent Nature

To gather preliminary insight on the self-assembly ability in solution of our probes, we firstly recorded their UV-vis spectra at the same concentration, in solution of different solvents, spanning a wide polarity range. In particular, we considered tetrahydrofuran, acetonitrile, dimethylsulfoxide, dimethylformamide, methanol and water. The spectra obtained for the two compounds, at 6.5 μM, are reported in Figure 1.

Looking at the spectra in Figure 1a, it can be observed that the UV-vis spectra of **NDI-Glu** shows two sharp peaks in the region 350–400 nm. The position of these bands and their intensity ratio depend on the solvent. In particular, the position of the shorter wavelength band shifts to higher values on increasing solvent polarity, going from 354 nm in solution of THF, to 357 nm in water, while the position of the longest wavelength band shifts from 375 nm–379 nm in the same solvents. This is an example of positive solvatochromism, which has been previously observed and reported also for other NDI-derivatives.[37,38] Changing the solvent also induces a slight change in the shape of the spectrum, with the two bands having comparable absorbances in MeOH and DMSO, while the longest wavelength transition is the most intense in water and DMF. Conversely, in the case of **NI-Glu**, the absorption spectra reported in Figure 1b show a marked dependence of the shape of the spectra from the solvent. More specifically, with the exception of water, the absorption spectra feature two distinct bands in the wavelength range comprised between 330 and 350 nm. In contrast, in aqueous solution the fine structure is lost and only one band appears, with maximum absorption at 344 nm. This observation could be a preliminary indication of supramolecular aggregation in water. This is consistent with literature reports on the supramolecular aggregation of 1,8-naphthalimide derivatives.[39]

To obtain further evidence on the aggregation of the two compounds in water, we recorded their emission spectra in solution of the same solvents, obtaining the spectra reported in Figure 1c–d. For **NDI-Glu**, Figure 1c, the shape of the spectra significantly changes as a function of the solvent, with a single emission band in all solvents except water (see enlarged spectrum in Figure S1), in which case, two distinct emission peaks can be observed, centered at 392 and 412 nm. In addition, emission intensity in THF is much higher, compared with others solvents. For the emission spectra of **NI-Glu**, reported in Figure 1d, we can observe a distinct behavior in water, with the most intense emission among the solvents considered, and a single band centered at 406 nm. This further supports the occurrence of aggregation in water for this compound, and the strong emission detected can derive from the occurrence of Aggregation Induced Emission (AIE), previously observed for related 1,8-naphthalimide derivatives in aqueous solution.[40,41]

In the other solvents, emission is significantly lower than in water, and the shape of the spectra changes as a function of the solvent. In particular, in the less polar THF and acetonitrile, a single emission band is present, centered at 390 and 393 nm respectively. This band shifts to higher wavelengths in more polar solvents, like DMF and DMSO, at 457 and 470 nm, respectively. Furthermore, only in DMSO a second emission band appears, centered at 532 nm.

Self-Assembly of the Fluorophores. The Effect Concentration

Given that these preliminary results hint at the occurrence of aggregation in water for both compounds, we went on to study their self-assembly in this solvent, by conducting concentration dependent spectroscopic analyses. In particular, we first recorded absorption spectra of both compounds in water, at increasing concentrations, from $1.9{\cdot}10^{-6}$ M–$9.3{\cdot}10^{-5}$ M in the presence of **NDI-Glu** and from $4.9{\cdot}10^{-6}$ M–$6.4{\cdot}10^{-5}$ M in the presence of **NI-Glu**. The spectra obtained are reported in Figure 2.

In the case of the spectra obtained for of **NDI-Glu**, reported in Figure 2a, no noticeable shift of adsorption bands occurs, although, as reported in the literature,[42] a clear indication of aggregation can be obtained by looking at the pronounced reduction of the molar extinction coefficient on increasing

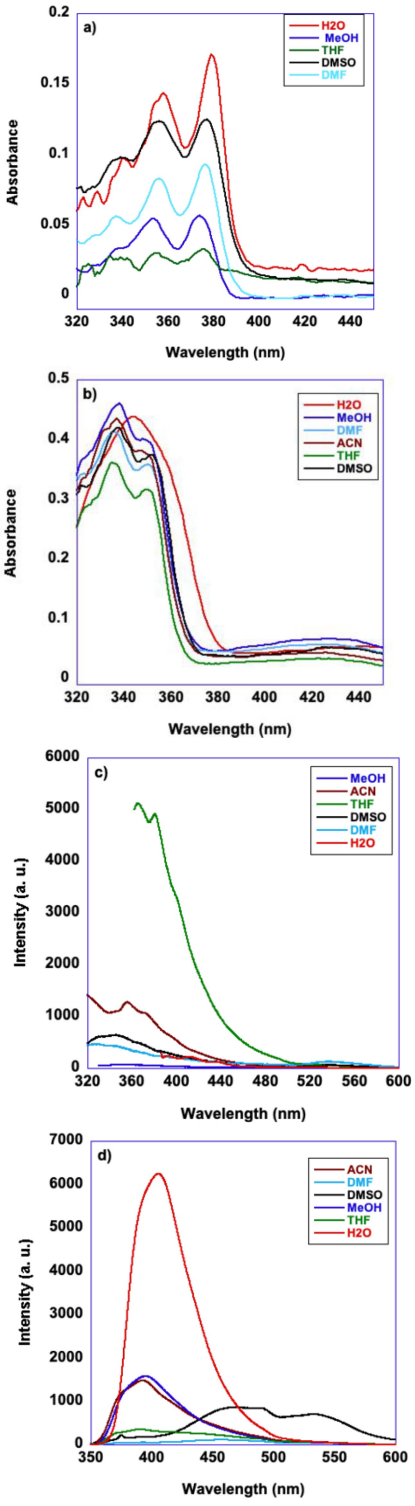

Figure 1. UV-vis spectra of 6.5 μM solutions of a) **NDI-Glu** and b) **NI-Glu** different solvents. Emission spectra of 6.5 μM solutions in different solvents of c) **NDI-Glu** and d) **NI-Glu.**

concentration, as reported in Figure S2. Conversely, in the case of **NI-Glu**, upon increasing concentration, the adsorption band shows a bathochromic shift, from 340 nm to 344 nm, suggesting the formation of *J*-aggregates.[40,43]

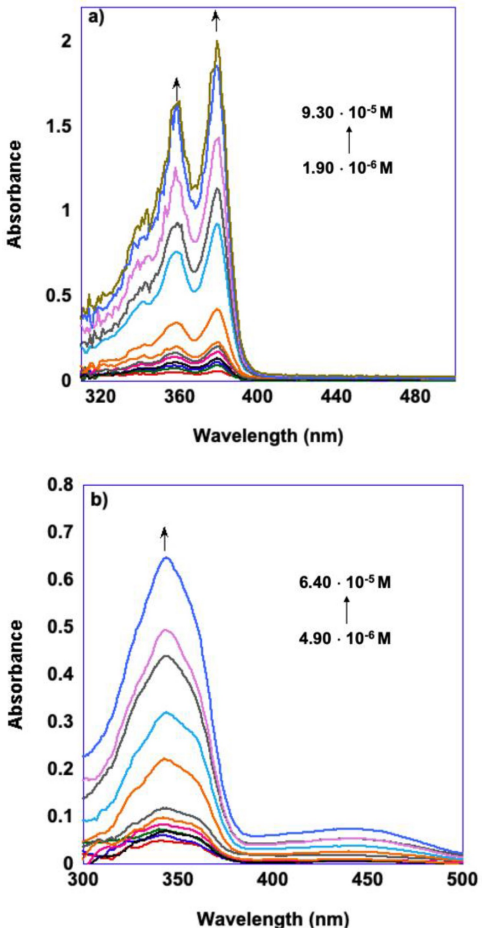

Figure 2. UV-vis spectra in aqueous solutions at increasing concentration of a) **NDI-Glu** and b) **NI-Glu**.

To obtain more information about the stability of the aggregates in aqueous solution for both compounds, and to study their aggregation mechanism, we carried out concentration dependent fluorescence spectroscopy measurements. The plots obtained are reported in Figure 3.

Examination of the spectra reported in Figure 3, points out that in both cases, no obvious quenching of fluorescence occurs on increasing concentration, which suggests the formation of emissive aggregates. In addition, for both compounds, emission intensity increases with concentration reaching a plateau value. However, a closer inspection of Figure 3a reveals that, in the case of **NDI-Glu**, increasing concentration brings substantial change in the shape of emission spectra. More specifically, while at the lowest concentration the spectrum displays only one band, centered at 437 nm, on increasing concentration two further bands appear, centered at 392 and 411 nm, and the previous band at 397 only appears as a shoulder. Moreover, upon increasing concentration a broad low energy emission band appears at 530 nm, which can be attributed to inter-chromophoric electronic communication at the excited states, between closely spaced NDI nuclei.[44,45]

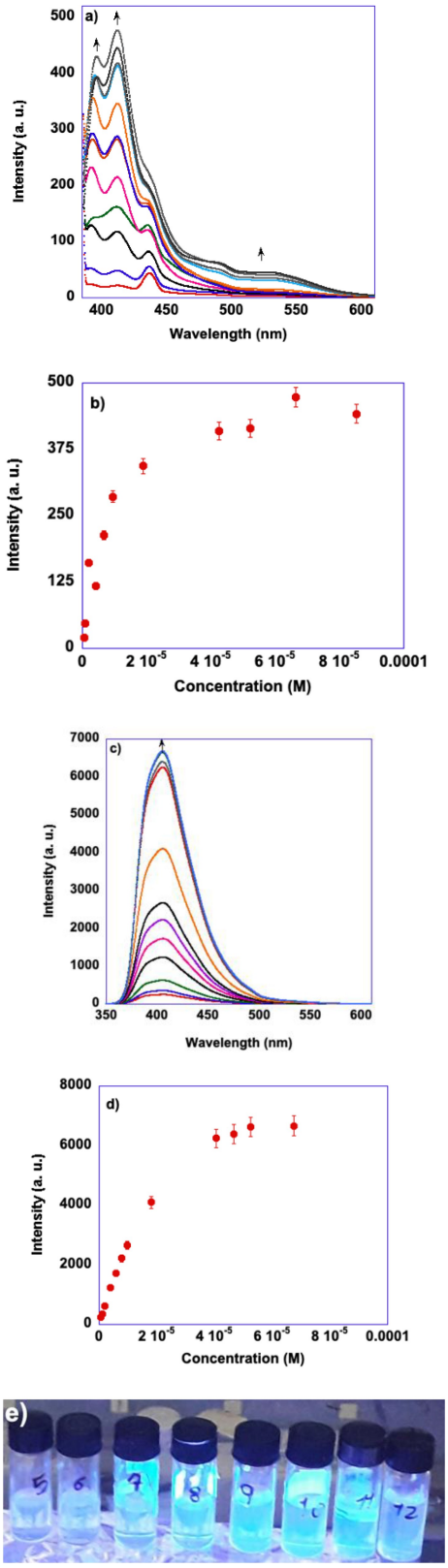

Figure 3. a) Concentration dependent fluorescence spectra in water for **NDI-Glu**, b) emission intensity at 411 nm for **NDI-Glu**, c) concentration dependent fluorescence spectra in water for **NI-Glu** and d) emission intensity at 404 nm for **NI-Glu**. Concentration of fluorophores ranged from $5.0{\cdot}10^{-7}$ M–$8.0{\cdot}10^{-5}$ M. λ_{exc} = 381 nm for **NDI-Glu** and 344 nm for **NI-Glu**, e) representative pictures of aqueous solutions of **NI-Glu** at increasing concentrations, under UV light.

From these measurements, we estimated the degree of aggregation, α_{agg}. *i.e.* the molar fraction of aggregates in solution expressed by equation 3,

$$\alpha_{agg} = \frac{[(I_C / C) - (I_{mon} / C_m)]}{[(I_{agg} / C_M) - (I_{mon} / C_m)]} \quad (3)$$

where C is the total concentration, I(C) is the emission intensity at a given concentration, I_{mon} is the emission intensity detected at the lowest concentration (C_m) which is assumed to be representative of the monomer and I_{agg} is the emission intensity measured at the highest concentration (C_M) which is in turn assumed to be representative of the aggregates.[33,46]

The plots obtained, reported in Figure 4, displayed a trend consistent with the isodesmic model of supramolecular aggregation.[47]

Accordingly, non-linear fit of the curve, by means of equation 4, based on this aggregation pathway,[48] allowed us to determine the equilibrium formation constants, K_{agg}.

$$\alpha_{agg} = 1 - \frac{2K_{agg}C + 1 - (4K_{agg}C + 1)^{0.5}}{2(K_{agg}C)^2} \quad (4)$$

The values of K_{agg} amounted to $(1.6 \pm 0.6)\ 10^6\ M^{-1}$ and $(3.0 \pm 0.9){\cdot}10^4\ M^{-1}$ for **NDI-Glu** and **NI-Glu**, respectively showing that **NDI-Glu** forms significantly more stable aggregates in water, compared with **NI-Glu**. The higher stability of the aggregates formed by **NDI-Glu** could be due to the presence of two glucamine functionalities on the molecule, compared with the only one present in **NI-Glu**. As a result, more hydrogen bonding sites are present in **NDI-Glu**, favouring interactions between the monomers.

Finally, we set out to obtain information about the thermodynamic properties relevant to the aggregation process in aqueous solution of both fluorophores, by carrying out temperature dependent UV-vis measurements at a fixed concentration, in the temperature range 25 °C ÷ 80 °C. However, as evidenced by the spectra reported in Figure S3, we detected no obvious change in the adsorption spectra, within the temperature range explored, suggesting the high stability of the aggregates formed.

Size, Morphology and Solid-State Emission of Aggregates

Subsequently, to investigate the size and morphology of the aggregates formed by the two fluorophores, we carried out dynamic light scattering (DLS) measurements, resonance light scattering (RLS), and recorded Scanning Electron Microscopy (SEM) images. In both cases, the samples were obtained from aqueous solutions at concentrations at which both fluorophores are mainly present in the aggregated form, equal to $6.15{\cdot}10^{-6}$ M **NDI-Glu** and $4.10{\cdot}10^{-5}$ M for **NI-Glu**.

Regarding DLS measurements, the plots of scattering intensity as a function of hydrodynamic diameter, Dh are reported in Figure 5.

The plots reported in Figure 5a show, in the aqueous solution of **NDI-Glu**, the occurrence of two distinct populations,

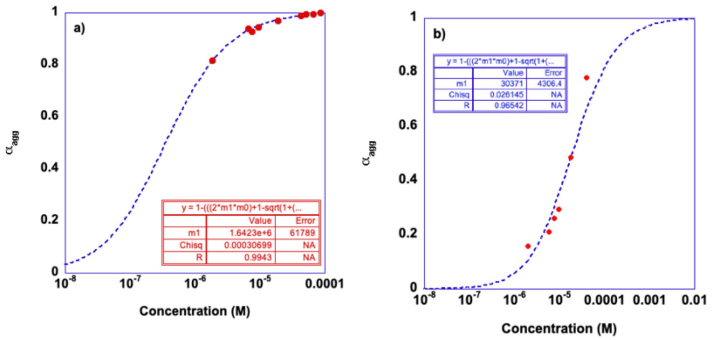

Figure 4. Plots of degree of aggregation α_{agg} as a function of concentration for a) **NDI-Glu**, and b) **NI-Glu**.

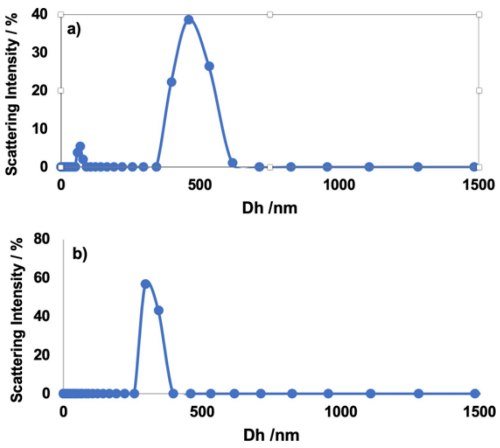

Figure 5. Plots relevant to the DLS measurements in aqueous solutions of a) **NDI-Glu** 6.15 10^{-6} M and b) **NI-Glu** 4.10 10^{-5} M.

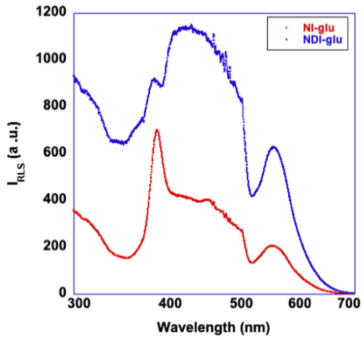

Figure 6. RLS spectra of aqueous solutions of aggregated for **NDI-Glu** ($6.15{\cdot}10^{-6}$ M) and b) **NI-Glu** ($4.10{\cdot}10^{-5}$ M).

with average hydrodynamic radius D_h of (60 ± 7) nm, and a majority population with an average D_h of (460 ± 50) nm. Conversely, for the aggregates of **NI-Glu**, DLS measurements show the occurrence of a single population, with an average hydrodynamic radius of (320 ± 20) nm. We obtained further information of the size of the aggregates by Resonance Light Scattering (RLS) measurements. This technique can be useful to investigate supramolecular aggregate systems formed by chromophore-containing molecules.[49] In particular, the intensity of the scattered light can be correlated to the size of aggregates in solution, with higher intensities indicating the occurrence of larger aggregates. As a result, RLS has been employed, for instance, to study a wide range of aggregates, including porphyrins,[50] ionic liquids[51,52] or gelation processes.[53,54]

Hence, we recorded the RLS spectrum of aqueous solutions of aggregated of both fluorophores, employing the same solutions used for the DLS measurements. The spectra obtained are reported in Figure 6.

The plots reported in Figure 6 clearly show that the intensity of scattered light is significantly higher in the case of **NDI-Glu** which indicated the occurrence of larger aggregates compared to **NI-Glu**. Interestingly, this is consistent with the evidence gathered by DLS measurements. In the case of systems displaying populations of aggregates of different size, the RLS intensity provides an averaged measurement, which again is consistent with the results of DLS investigations.

Finally, we characterized the morphology of the aggregates by scanning Electron Microscopy (SEM). Samples were obtained by slow evaporation, at room temperature, of solutions of aggregates, at the same concentration used for the previous investigation, on the aluminum stub. As a consequence, drying effects may occur, which make the aggregates appear larger, when probed by the microscope.[55] This is the reason why we only use the SEM images to gather qualitative information, pertaining only the morphology of the aggregates and not the size. The SEM images obtained are reported in Figure 7.

Examination of the SEM images shows a very different morphology for the aggregates formed by the two compounds. In particular, the aggregates formed by **NDI-Glu** (Figure 7a) appear as irregular shaped objects, whereas the ones formed by **NI-Glu** display a network of filamentous structures, arranged in a cobweb-like fashion (Figure 7b). Once again, the more extended aggregates detected for **NDI-Glu**, even at a lower concentration, could be ascribed to the presence of a second D-glucamine moiety, providing more possible sites of interaction among monomers, compared with **NI-Glu**, which bears only one glucamine moiety.

Finally, we determined the fluorescence spectra of both aggregates systems in the solid state, to investigate whether the fluorescence capability is retained also in the solid state. These spectra were recorded on thin films obtained by evaporation of aqueous solutions of **NDI-Glu** and **NI-Glu**, at the

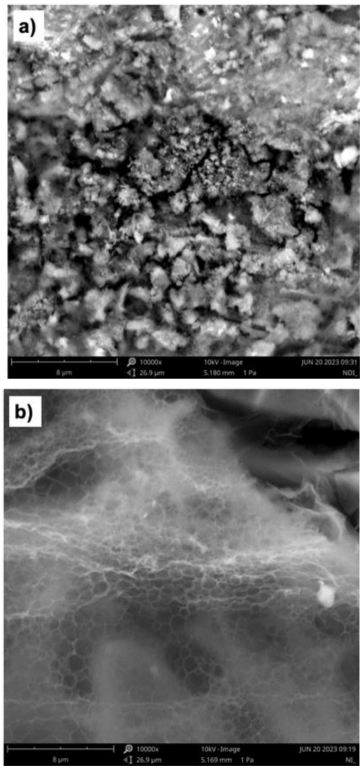

Figure 7. SEM images relevant to the aggregated in aqueous solutions formed by a) **NDI-Glu** and b) **NI-Glu**. Samples obtained from evaporation of **NDI-Glu** ($6.15{\cdot}10^{-6}$ M) and b) **NI-Glu** ($4.10{\cdot}10^{-5}$ M) aqueous solutions.

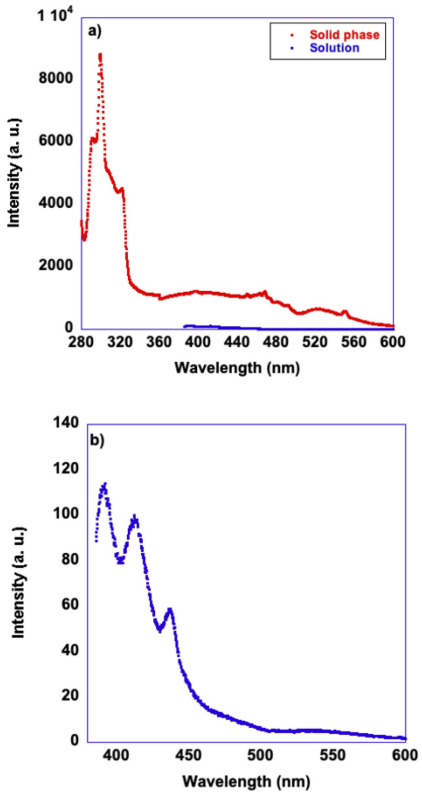

Figure 8. a) Superimposed solid phase and solution spectra of **NDI-Glu** and b) enlarged solution phase spectrum.

same concentrations used for the previous investigations, at which both compounds are mainly present in aggregated form. In the solid state, no fluorescence was detected for **NI-Glu**, while the results obtained for **NDI-Glu** are reported in Figure 8.

In this latter case, as can be seen in Figure 8, the aggregates present in the solid state are much more emissive than those in solution. NDI-based molecules generally show quenching of emission in the solid state, due to strong stacking interactions, and the occurrence of emission from aggregates in the solid state is less frequent.[56,57] In our case, likely the bulky hydroxylated chains of D-glucamine interefere with the stacking of NDI cores, allowing fluorescence emission. In addition, from the spectra reported in Figure 8, it is apparent that emission in the solid state is blue-shifted compared with emission in solution. As reported in the literature, this can be due to lower reorganization energy in aggregate than the solution phase.[58]

Sensing of Pharmaceutically Active Compounds

After characterizing the self-assembly and aggregates formed by **NDI-Glu** and **NI-Glu**, we investigated the possibility of using both compounds as sensors for drugs in aqueous solutions. To this aim, we conducted fluorescence measurements of aqueous solutions containing fixed concentration of **NDI-Glu** or **NI-Glu**, and increasing amounts of drugs. The drugs considered were nalidixic acid, ciprofloxacin, diclofenac sodium salt and carbamazepine. To ensure that no overlap occurs at the absorption spectra of drugs and fluorophores, we recorded the UV-vis spectra of **NI-Glu** and **NDI-Glu** and the ones of the drugs in water. The concentrations of fluorophore used were the ones used in the measurements (see later) while the spectra of the drugs were acquired at the highest concentration used in the sensing measurements. The spectra are reported in Figure S4, and show no overlap between drugs and fluorophore and absorbance of drugs is always negligible at $\lambda_{exc.}$ Hence, the variations of emissions observed upon increasing the concentrations of drugs is only due to the fluorophores and no charge transfer processes between fluorophore and analyte occurs. Then, we carried out the fluorescence measurements upon varying the concentrations of drugs. For the sake of clarity, we will describe the results obtained with **NDI-Glu** first, and subsequently, the ones obtained in the presence of **NI-Glu**.

Sensing of Drugs in the Presence of NDI-Glu

All the measurements were carried out using a fixed concentration of **NDI-Glu** of $6.0{\cdot}10^{-6}$ M, while the concentration of drugs was comprised between $1.0{\cdot}10^{-8}$ M and $9.0{\cdot}10^{-6}$ M. Representative plots of the spectra obtained are reported in Figure 9a, while the other ones are reported in Figures AS-7.

The spectra reported in Figure 9a show that the presence of nalidixic acid induces an enhancement of fluorescence emission. In particular, the plot of emission intensity at 440 nm, as a function of drug concentration (Figure 9b) shows that emission

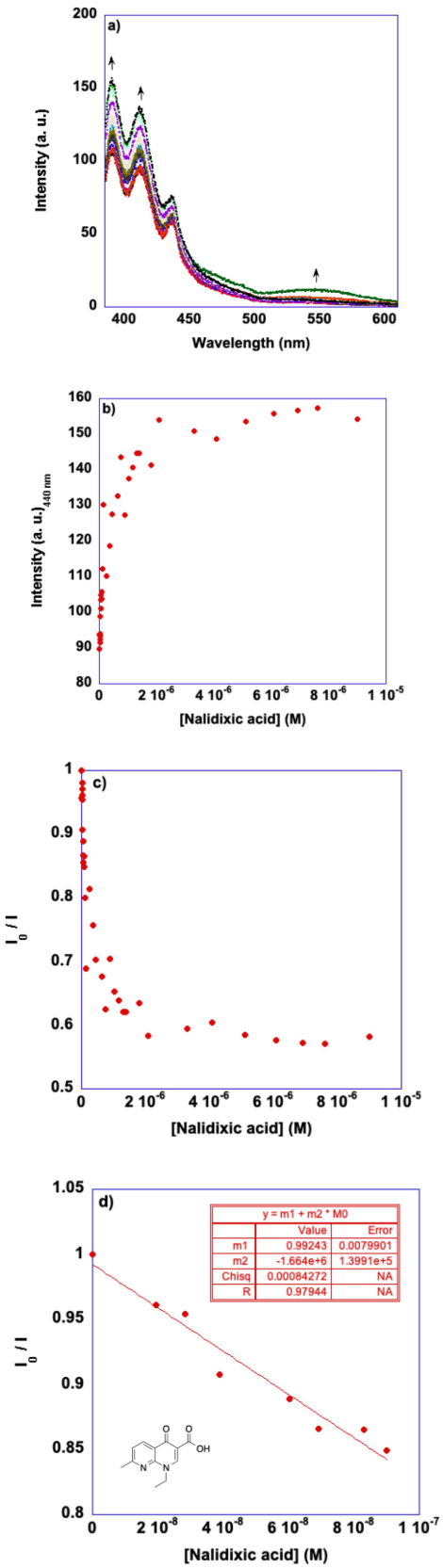

Figure 9. a) Fluorescence spectra of aqueous solutions of **NDI-Glu** ($6.0{\cdot}10^{-6}$ M) in the presence of increasing amounts of nalidixic acid, b) emission intensity at 440 nm as a function of drug concentration, c) emission enhancement ratio as a function of concentrations **NDI-Glu**, d) fit of linear tract of I_0/I as a function of concentration.

intensity increases upon reaching a plateau value. In addition, no change in the shape of the spectra is detected, upon increasing drug concentration. Subsequently, we plotted the emission enhancement ratio, I_0/I, where I_0 is the emission intensity of **NDI-Glu** in the absence of drug, and I the emission of the sample, obtaining the plot reported in Figure 9c. This plot shows a non-linear trend, in which we can observe a practically linear response of the emission enhancement ratio at low concentration of drug. Consequently, we applied a linear regression to this tract obtaining the results reported in Figure 9d. In this case, the linear regression analysis evidenced a good correlation of I_0/I, in the concentration range comprised between 0 and $1.0{\cdot}10^{-7}$ M. On the light of this, we applied equation (1) and (2) (see Supporting information) to determine the Limit of Detection (LOD) and Limit of Quantification (LOQ) of nalidixic acid, which fall in the sub-micromolar range. Similar trends were found in the case of the other drugs, and the same treatment allowed us to obtain the values of LOD and LOQ reported in Table 1.

The results reported in Table 1, show that the emission of **NDI-Glu** in water is sensitive to the presence of all the drugs at very low concentrations. In particular, the trend of LOD and LOQ follows the order: nalidixic acid, $<$ carbamazepine $\ll$ ciprofloxacin $\approx$ diclofenac. This suggests that hydrogen bonding plays a marginal role in the interaction between **NDI-Glu** and the drugs, since the probe appears markedly sensitive to the presence of carbamazepine, which is the only drugs devoid of charged sites, among the ones considered in this work. It is indeed important to remember that, as reported in the literature,[29,30] nalidixic acid and ciprofloxacin are predominantly present in zwitterionic form in aqueous solution, and so they bear a carboxylate anion and an ammonium cationic site. Consequently, the sensitivity of the emission of this probe to the presence of the drugs can be due to the concomitant action of different factors like the extension of the π -surface and molecular rigidity.

Sensing of Drugs in the Presence of NI-Glu

The same approach described above, was followed to study the sensing ability of aggregates of **NI-Glu** towards drugs in aqueous solutions. In this case, the concentration of **NI-Glu** in the samples was equal to $4.0{\cdot}10^{-5}$ M, while typical concentrations of drugs in the samples ranged from $1.0{\cdot}10^{-8}$ M–$3.0{\cdot}10^{-4}$ M. Representative plots relevant to such measurements

Table 1. Values of LOD and LOQ for drugs obtained in the presence of **NDI-Glu** as sensor.

Drug	LOD (M)	LOQ (M)
Nalidixic acid	$(1.5\pm0.1){\cdot}10^{-8}$	$(4.8\pm0.4){\cdot}10^{-8}$
Ciprofloxacin	$(1.12\pm0.09){\cdot}10^{-7}$	$(3.4\pm0.3){\cdot}10^{-7}$
Diclofenac sodium salt	$(1.46\pm0.07){\cdot}10^{-7}$	$(4.4\pm0.2){\cdot}10^{-7}$
Carbamazepine	$(2.1\pm0.2){\cdot}10^{-8}$	$(6.5\pm0.6){\cdot}10^{-8}$

are reported in Figure 10, while the other ones are reported in Figures S8–S9.

Differently from what we described above, the emission of **NI-Glu** undergoes quenching, upon increasing concentration of drugs. In addition, no significant variation in emission fluorescence was detected in the presence of carbamazepine. The values of LOD and LOQ, determined as described previously, are reported in Table 2.

In general, all the values obtained in the presence of **NI-Glu** are much higher than the corresponding ones observed in the presence of **NDI-Glu**, suggesting a higher sensitivity of this latter towards the drugs considered. A closer look at the LOD and LOQ values reported in Table 2 shows that they increase along the sequence: diclofenac < ciprofloxacin < nalidixic acid, which is practically opposite to the one detected in the presence of **NDI-Glu**, hinting at a significant difference in the mode of interaction between the probes and the drug. This is further supported by the inability of **NI-Glu** to sense carbamazepine, which is the only drug devoid of charged sites among the ones considered. Consequently, we could hypothesize that hydrogen bond plays a role within the interaction between **NI-Glu** and the drugs, unlike what happens in the case of **NDI-Glu**. In a subsequent section we will deal with the interaction mode between **NI-Glu** and drugs.

Since both probes are sensitive to the presence of more than one drug, it is important to address the issue of selectivity. If we consider as a first guide for both fluorophores, the ratios of the LODs for the drugs to which they are least and most sensitive, these amount to 9.7 and 960 for **NDI-Glu** and **NI-Glu**, respectively. These suggests that both probes could in principle achieve a certain selectivity and tolerate moderate amounts of another drug. To verify this hypothesis, we carried out fluorescence experiments aimed at investigating how emission intensity of the probes while detecting one drug, are affected by the presence of 0.1 eq and 1 eq of a second drug. In particular, we determined the relative emission intensities of samples of **NDI-Glu** with nalidixic acid, in the presence of 0.1 eq and 1 eq of diclofenac, as well as **NI-Glu** with diclofenac, in the presence of nalidixic acid. Concentrations were chosen to fall within the linear response range. The results obtained are reported in Figure 11.

The results reported in Figure 11 show that there is no significant variation of the emission intensity of the samples, upon addition of 0.1 eq and 1 eq of the second drug. In particular, values of relative intensities obtained were (1.12 ± 0.08) and (1.00 ± 0.01) upon adding 0.1 eq and 1 eq of DCF to the solution of **NDI-Glu** and NA. For **NI-Glu** in the presence of DCF, relative intensities found were (0.95 ± 0.01) and (0.99 ± 0.01) upon adding 0.1 eq and 1 eq of NA, respectively. Consequently, both probes can tolerate the presence of moderate amounts of a second drug without altering significantly the measurements, showing that a certain selectivity can be achieved.

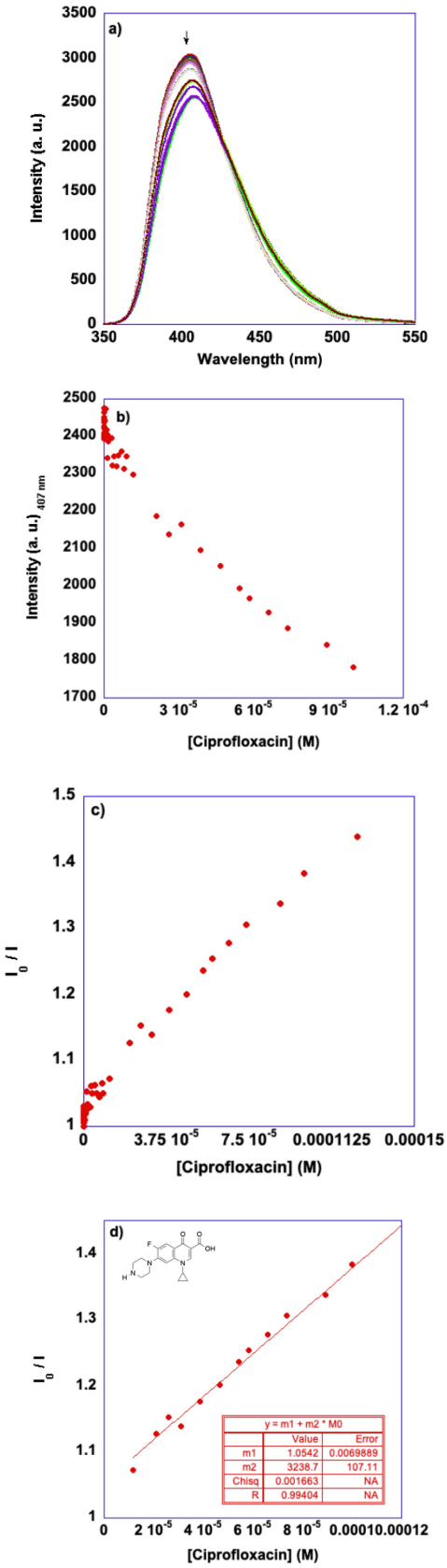

Figure 10. a) Fluorescence spectra of aqueous solutions of **NI-Glu** ($4.0 \cdot 10^{-5}$ M) in the presence of increasing amounts of ciprofloxacin, b) emission intensity at 407 nm as a function of drug concentration, c) emission enhancement ratio as a function of concentrations **Ni-Glu** and d) fit of linear tract of I_0/I as a function of concentration.

Table 2. Values of LOD and LOQ for drugs obtained in the presence of **NI-Glu** as sensor.

Drug	LOD (M)	LOQ (M)
Nalidixic acid	$(2.5 \pm 0.2)\cdot10^{-5}$	$(7.5 \pm 0.6)\cdot10^{-5}$
Ciprofloxacin	$(7.1 \pm 0.2)\cdot10^{-6}$	$(2.16 \pm 0.07)\cdot10^{-5}$
Diclofenac sodium salt	$(2.6 \pm 0.4)\cdot10^{-8}$	$(8.6 \pm 1.3)\cdot10^{-8}$

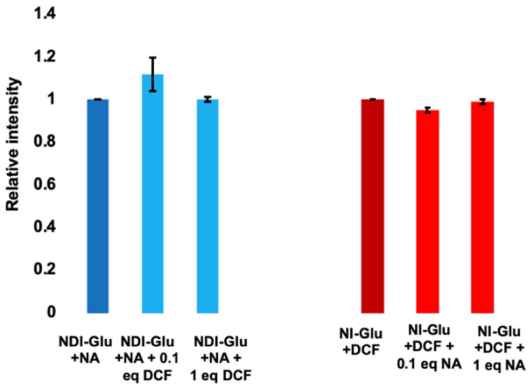

Figure 11. Relative fluorescence intensities in the presence of a second drug in the sample. On the left, intesities relative to an aqueous solution of **NDI-Glu** (6.0 μM) + NA (6.0 μM), upon addition of 0.1 eq and 1 eq of DCF. On the right, intesities relative to an aqueous solution of **NI-Glu** ($4.0\cdot10^{-5}$ M) + DCF ($6.0\ 10^{-8}$ M), upon addition of 0.1 eq and 1 eq of NA. Experiments were performed in triplicate. Equivalents are relative to the probes.

Table 3. Chemical shifts of **NI-Glu**, DCF and their mixtures in DMSO–D6.

δ NDI-Glu (ppm)	δ DCF (ppm)	δ NDI-Glu + 0.1 eq DCF (ppm)	δ NDI-Glu + 1 eq DCF (ppm)
	10.27	9.52	9.96
8.59		8.54	8.55
8.44		8.40	8.38
8.04		8.00	7.96
	7.43	7.41	7.41
	7.05	7.06	7.05
	6.91	6.92	6.94
	6.72	6.74	6.74
	6.23	6.20	6.23
4.76		4.49	4.50
4.51		4.46	4.47
4.37		4.04	4.05
4.03		3.93	3.93
3.94		3.69	3.71

Interaction between Probes and Drugs

On the grounds of all these results, it could be interesting to gather information regarding the interaction mode between the probes and drugs. To this aim, we firstly recorded the solid-state spectra of both probes in the presence of 1 eq of the drug to which they are most sensitive, namely NA for **NDI-Glu** and DCF for **NI-Glu**. However, the spectra obtained, reported in Figure S11 showed no obvious change in signal positions. It is important to remember however that interactions in solid state are very different compared with the solution state. For this reason, we went on to gather this information by recording the ^{1}H NMR spectra of the probes in the presence of 0.1 eq and 1 eq of the drugs chosen.

The change in signal position upon adding the drug can give evidence about the occurrence of π-π or hydrogen bond interactions. Unfortunately, for solubility reasons, we could conduct this investigation only for **NI-Glu** and only in DMSO–D6. We are aware that the situation in DMSO could be different from the one in water, but nonetheless we are reasonably confident that valuable information can be obtained. The spectra of **NI-Glu** in the presence of 0.1 eq and 1 eq of DCF are reported in Figure S12, while in Table 3, we report the chemical shift values of the most affected signals.

Results reported in Table 3, shows that upon adding the drug, the signals of the aromatic protons of **NI-Glu** (8.59–8.44 ppm) undergo upfield shift, while the aromatic protons of DCF are unaltered. Also, the N–H proton of DCF (10.27 ppm) moves significantly upfield. This can suggest the occurrence of π-π interactions (see later).

Conversely, the aliphatic and hydroxyl protons of **NI-Glu**, relevant to the glucamine moiety, move significantly upfield. This can be attributed to shielding effect of the aromatic rings, which overcomes potential hydrogen bonding. In this situation, hydrogen bonding interaction should involve the carboxylate moiety of DCF. However, it is not possible to prove unequivocally the occurrence of hydrogen bonding between fluorophore and DCF.

Based on these findings, we propose that DCF interposes between the NI-rings in the aggregates, in the way depicted schematically in Figure 12.

This agrees with the upfield shifts of the aromatic protons of **NI-Glu** and N–H proton of DCF, due to their positioning within the shielding cone of the aromatic rings. On the other hand, the aromatic protons of DCF are outside this shielding zone and do not undergo significant shift. Conversely, the occurrence of hydrogen bonding could not be proved unequivocally. This could be explained by absence of hydrogen bonding. Alternatively, if hydrogen bonding occurs, the expected downfield shift is overcome by the shielding effect by the aromatic rings. It is worth noting that the chemical shift of the N–H proton on DCF, increases from 9.52–9.96 ppm as the

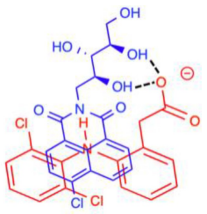

Figure 12. Schematic depiction of possible interaction mode between NI-Glu and DCF. For the sake of clarity, the structures are not in scale.

amount of DCF increases from 0.1 eq to 1 eq. This can be explained by considering that when DCF interposes within the NI-rings it can reduce the interaction between NI-units favoring a partial disassembly. This is more evident when the amount of DCF raises to 1 eq, in which case the fraction of "free" DCF increases, giving a chemical shift that is the average of the ones of DCF within the aggregates and "free". Based on all these considerations, we propose in Figure 13 a schematic representation for the mechanism of sensing.

In our hypothesis, NI-aggregates can interact with drugs which interpose between the NI-rings, determining partial disassembly and as a consequence, fluorescence quenching.

Finally, to assess the performance of our system we report below Table 4, comparing our best results, with recent literature examples, dealing with fluorescent sensing of the same drug in aqueous solutions.

A first glance at the results reported in Table 4 shows that the performance of our best our best sensor probe, **NDI-Glu**, is perfectly in line, in some cases superior in terms of LOD and LOQ, to fluorescent sensors used to detect the same drugs, recently reported in the literature. In particular, among various systems, carbon dots have recently emerged as interesting sensing probes, due to their fluorescence.[67]

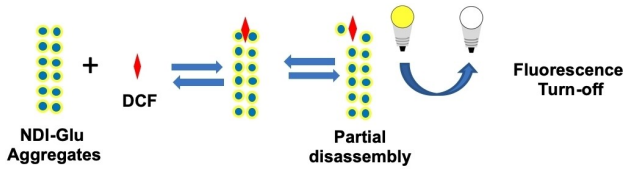

Figure 13. Schematic depiction of sensing mechanism by **NI-Glu.**

Table 4. Comparison of LOD of NDI-Glu and literature system for sensing of drugs in water.

Sensor	Drug	LOD (μM)
NDI-Glu[a]	Carbamazepine	(0.021 ± 0.002)
N-doped carbon dots[59]		8.16
MOF/carbon dots composite[60]		$1.7{\cdot}10^{-3}$
Carbon nitride-CuS composite[61]		$1.3{\cdot}10^{-2}$
NDI-Glu[a]	Diclofenac	(0.146 ± 0.007)
Piezoelectric immunosensor[62]		$9.5{\cdot}10^{-3}$
β-cyclodextrin nanosponge[63]		0.92
NDI-Glu[a]	Ciprofloxacin	(0.112 ± 0.007)
Carbon-CdTe quantum dots composite[64]		0.09
Porous organic framework[65]		0.019
NDI-Glu[a]	Nalidixic acid	(0.015 ± 0.001)
Ag–Cu(II) nanoclusters[66]		$4.7{\cdot}10^{-4}$

Regarding the sensing of diclofenac, **NDI-Glu** has a much lower detection limit as compared to a system employing N-doped carbon dots.[59] In addition, the performance of **NDI-Glu** is comparable to the one of a carbon nitride-CuS composite,[60] while it is outperformed by a system using a composite carbon dot-doped MOF.[61] Similar conclusions can be drawn by examining the results in the presence of ciprofloxacin, where our **NDI-Glu** probe has a detection limit comparable to the one of a functionalized β-cyclodextrin nanosponge,[63] whereas a piezoelectric immunosensor achieves a much more sensitive level of detection.[62] Despite its simple preparation, the performance of **NDI-Glu** in the presence of ciprofloxacin equalizes the one of more complex systems, like nanocomposites of carbon and quantum dots.[64] On the other hand, **NDI-Glu** shows a worse performance, compared with a porous organic framework functionalized with emissive moieties.[65] Finally, comparatively fewer fluorescent probes are reported for nalidixic acid. In this case the performance of our probe is inferior to the one of Ag–Cu(II) nanoclusters, which show also high sensitivity to the detection of other fluoroquinolones in water in the sub-nanomolar range.[66]

Conclusions

With the aim to design fast and selective systems for detection of EP in water bodies, we have synthesized two D-glucamine-functionalized fluorophores bearing the 1,8-naphthalimide (**NI-Glu**) and the naphthalene diimide (**NDI-Glu**) nuclei. We studied the self-assembly of both compounds, finding that they aggregate in aqueous solution via an isodesmic pathway, with **NDI-Glu** forming more stable and larger aggregated, as probed by fluorescence, DLS and RLS measurements. We also observed a different morphology of the aggregates formed by the two compounds by SEM investigation, showing a filamentous structure for the ones formed by **NI-Glu** and a more compact texture for the aggregates formed by **NDI-Glu**. Then, we studied the ability of both compounds to sense drugs of different classes like ciprofloxacin, diclofenac, carbamazepine and nalidixic acid. We found that both compounds show significant variation of emission intensity in the presence of increasing concentrations of drugs. In particular, **NDI-Glu** exhibited enhancement of emission, whereas **NI-Glu** underwent quenching of fluorescence. The two probes showed different sensitivities to structural features of the drugs, with **NDI-Glu** more sensitive to drugs featuring larger π-surface are and molecular rigidity, whereas **NI-Glu** was more sensitive to drugs bearing charged sites. **NDI-Glu** proved the most sensitive probe, with LOD in the sub-micromolar range for all drugs ($0.015\ \mu M < LOD < 0.146\ \mu M$). In addition, NMR investigations allowed us to put forward a mechanistic hypothesis for the sensing by **NI-Glu** aggregates.

Comparison of the sensing ability of **NDI-Glu** with different sensory systems reported in the literature shows that our probe has a competitive performance, with the advantage of a simpler structure and preparation, outperforming more complex systems like N-doped carbon dots or α -cyclodextrin sponges.

Experimental Section

Materials

Methanol, ethanol, dimethylformamide, acetonitrile, dimethylsulfoxide, D-glucamine, 4-chloro-1,8-naphthalic anhydride, 1,4,5,8-naphthalenetetracarboxylic dianhydride, carbamazepine, diclofenac sodium salt, ciprofloxacin and nalidixic acid were obtained from commercial sources and used without further purification.

FT-IR spectra of pure fluorophores were recorded on nujol mull, while the samples relevant to ascertaining interactions between probed and drugs were prepared as KBr pellets.

NMR spectra were acquired on a Brucker instrument working at 400 MHz. Chemical shift are expressed in ppm relative to TMS.

Synthesis of Fluorophores

The two fluorophores, **NDI-Glu** and **NI-Glu**, were prepared by a modification of procedures reported in literature.[31–33]

In particular, 1 g of the relevant anhydride and the suitable amount of D-glucamine (1 eq. for NI-Glu and 2 eq. for NDI-Glu) was dissolved in 20 mL of dimethylformamide and the resulting mixture was heated at 110 °C, under stirring for 72 h. Subsequently, the reaction mixture was allowed to cool at room temperature, and the solvent was removed by evaporation. The solid residue was then washed with portions of acetone (3×5 mL), deionized water (3×5 mL) and dried by evaporating at reduced pressure.

NI-Glu

Yellow solid; Yield: 83 %; m.p. 117–120 °C. FT-IR (nujol mull): 3355, 1653 cm^{-1}. ^{1}H-NMR (400 MHz, DMSO–D6) δ: 3.49 (m, 3H), 3.59 (m, 1H), 3.68 (m, 1H), 3.94 (dd, J_1 = 12 Hz, J_2 = 4 Hz, 1H), 4.03 (sext, J = 4 Hz, 1H), 4.34 (m, 2H), 4.37 (d, J = 8 Hz, 1H), 4.51 (m, 2H), 4.76 (d, J = 8 Hz, 1H), 8.04 (m, 2H), 8.44 (d, J = 8 Hz, 1H), 8.59 (m, 2H) ppm. ^{13}C-NMR (400 MHz, DMSO–D6) δ (ppm): 163.7, 163.5, 137.6, 131.9, 131.2, 130.2, 129.0, 128.8, 128.1, 128.0, 123.5, 122.2, 72.6, 71.9, 70.6, 70.3, 63.8, 43.5 ppm. Elemental Anal. Calcd. for $C_{18}H_{18}ClNO_7$ (395.8): C, 54.6; H, 4.86; N, 4.58. Found: C, 54.3; H, 5.0; N, 4.3.

NDI-Glu

Gray solid; Yield: 71 %; m.p. 244–248 °C. FT-IR (nujol mull): 3361, 1645.2 cm^{-1}. ^{1}H-NMR (400 MHz, $CDCl_3$) δ: 3.71–3.50 (m, 9H), 4.06–3.98 (m, 4H), 4.52–4.33 (m, 11H), 4.83 (s, 2H), 8.64 (s, 4H) ppm. ^{13}C-NMR (400 MHz, $CDCl_3$) δ : 163.4, 130.8, 126.9, 126.6, 72.5, 72.0, 70.7, 70.1, 63.8, 43.8 ppm. Elemental Anal. Calcd. for $C_{26}H_{30}N_2O_{14}$ (594.2): C, 52.52; H, 4.71; N, 5.09. Found: C, 52.2; H, 5.0; N, 5.2.

Dynamic Light Scattering

DLS measurements were performed by using a Zetasizer Nano ZS instrument at a fixed scattering angle of 173°. A He/Ne laser (4 mW) with a wavelength of λ = 633 nm was used. The normalized correlation function of the electric field was analyzed by using a computer algorithm of the Malvern software, which performs an inverse Laplace transformation (ILT). The ILT analysis yields an intensity-weighted relaxation time distribution N, which can be transformed to an intensity-weighted particle size distribution based on the apparent hydrodynamic diameter by using the Stokes-Einstein equation and the solvent viscosity at the corresponding temperature.

RLS Measurements

RLS measurements were carried out with a spectrofluorometer employing a synchronous scanning mode in which the emission and excitation monochromators were preset to identical wavelengths. RLS spectra were recorded from 300–700 nm, with both excitation and emission slit widths set at 2.5 nm. Spectra were obtained after 15 accumulations.

SEM Images

Samples for SEM images were prepared by casting on an aluminum stub 50 μL of an aqueous solution of each fluorophore, and the solvent was removed by evaporation at room temperature. Then, SEM images were recorded on a PRO X PHENOM electronic scanning microscope, operating at 5 KV.

UV-vis and Fluorescence Spectra

Samples for UV-vis and fluorescence spectra were prepared by dilution of stock solutions of **NI-Glu** or **NDI-Glu** in methanol. The suitable volume of solution was withdrawn and then the solvent was removed by evaporation under reduced pressure. Then, the residue was dissolved in the suitable volume of water to obtain the desired concentration. All the solution were limpid and stable after this treatment. UV-vis and fluorescence spectra were recorded using quarts cuvettes (l = 1 cm and 0.2 cm for UV-vis and fluorescence measurements, respectively). Concentration of samples for UV-vis spectra ranged from $1.9{\cdot}10^{-6}$ M–$9.0{\cdot}10^{-5}$ M, while the ones for fluorescence spectra ranged from $5.0{\cdot}10^{-7}$ M–$8.0{\cdot}10^{-5}$ M. Fluorescence spectra were obtained by excitation at the λ_{max} obtained from excitation spectra. Excitation and emission spectra were recorded by setting excitation and emission slid width to 2.5 nm, after 10 accumulations. Fluorescence spectra recorded in aqueous solutions were obtained at λ_{exc} = 381 nm for **NDI-Glu** and 344 nm for **NI-Glu**.

Temperature-dependent UV-vis spectra were recorded on an instrument equipped with a Peltier temperature controller, able to keep temperature constant within ±0.1 °C

Solid State Fluorescence Spectra

Solid-state fluorescence spectra were recorded from films obtained by casting 200 μL of aqueous solutions of fluorophore ($4.3{\cdot}10^{-5}$ M for NI-Glu and $8.8{\cdot}10^{-6}$ M for NDI -Glu) onto quartz plates. The solvent was removed by evaporation at room temperature, obtaining a solid thin film. To ensure a meaningful comparison between solid- and solution phase spectra, the excitation spectra were recorded for each sample. Emission spectra were obtained by exciting the samples at the λ_{max} obtained by excitation spectra.

Fluorescence Sensing of Drugs

Sensing measurements for the detection of drugs in aqueous solutions were carried out by recording fluorescence spectra of aqueous solutions containing a fixed amount of fluorescent probe ($6.0{\cdot}10^{-6}$ M for NDI-Glu and $4.0{\cdot}10^{-5}$ M for NI-Glu) and increasing amounts of drugs. Drug concentrations were comprised between $1.0{\cdot}10^{-8}$ M and 9.0 10^{-6} M in the presence of NDI-Glu and between $1.0{\cdot}10^{-8}$ M and $3.0{\cdot}10^{-4}$ M in the presence of NI-Glu. Solutions were prepared by dilution of stock solutions as previously described. For each measurement, at least 40 solutions were prepared and the relevant emission spectra were obtained as described above. Then, for each sample, the ratio I_0/I was determined where I_0 is the

maximum intensity emission of the solution containing no drug and I is emission intensity in the presence of a given amount of drug. This ratio was plotted as a function of the concentration of drug and, whenever present, the linear tract of this plot was fitted by linear regression analysis, to obtain the limit of detection (LOD) and the limits of quantification (LOQ),[68] by means of Equations (1 and 2)

$$LOD = 3 \cdot \frac{S_y}{s} \quad (1)$$

$$LOQ = 10 \cdot \frac{S_y}{s} \quad (2)$$

where Sy is the error on the intercept and s is the slope of the curve.

Author Contributions

Salvatore Marullo: writing, original draft, visualization; **Riccardo Arena**: investigation: sensing and self-assembly experiments; **Giuseppe Lazzara** and **Giuseppe Cavallaro**: investigation: dynamic light scattering; **Michele Cacioppo**: review and editing; **Francesca D'Anna**: conceptualization, writing, review and editing, supervision and funding acquisition.

Acknowledgements

This work was supported by SiciliAn MicronanOTecH Research And Innovation CEnter "SAMOTHRACE" (MUR, PNRR–M4C2, ECS 00000022), spoke 3 - Università degli Studi di Palermo "S2-COMMs - Micro and Nanotechnologies for Smart & Sustainable Communities". The funding sources had no involvement in study design; collection, analysis and interpretation of data; writing of the report and in the decision to submit the article for publication. Open Access publishing facilitated by Università degli Studi di Palermo, as part of the Wiley - CRUI-CARE agreement.

Conflict of Interests

The authors declare no conflict of interest.

Data Availability Statement

The data that support the findings of this study are available in the supplementary material of this article.

Keywords: Aggregation · D-Glucamine · 1,8-naphthalimide · Naphthalene diimide · Sensing · Water monitoring · fluorescence

[1] C. G. Daughton, *Environ. Impact Assess. Rev.* **2004**, *24*, 711–732.
[2] Y. Tang, M. Yin, W. Yang, H. Li, Y. Zhong, L. Mo, Y. Liang, X. Ma, X. Sun, *Water Environ. Res.* **2019**, *91*, 984–991.
[3] A. Rastogi, M. K. Tiwari, M. M. Ghangrekar, *J. Environ. Manage.* **2021**, *300*, 113694.
[4] L. H. M. L. M. Santos, A. N. Araújo, A. Fachini, A. Pena, C. Delerue-Matos, M. C. B. S. M. Montenegro, *J. Hazard. Mater.* **2010**, *175*, 45–95.
[5] R. Delli Compagni, F. Polesel, K. J. F. von Borries, Z. Zhang, A. Turolla, M. Antonelli, L. Vezzaro, *Water Res.* **2020**, *184*, 116097.
[6] W. C. Chong, Y. L. Choo, C. H. Koo, Y. L. Pang, S. O. Lai, *AIP Conf. Proc.* **2019**, 020005.
[7] M. Gutiérrez, V. Grillini, D. Mutavdžić Pavlović, P. Verlicchi, *Sci. Total Environ.* **2021**, *790*, 148050.
[8] M. S. Díaz-Cruz, D. Barceló, *Chemosphere* **2008**, *72*, 333–342.
[9] L. Walekar, T. Dutta, P. Kumar, Y. S. Ok, S. Pawar, A. Deep, K.-H. Kim, *TrAC Trends Anal. Chem.* **2017**, *97*, 458–467.
[10] J. Krämer, R. Kang, L. M. Grimm, L. De Cola, P. Picchetti, F. Biedermann, *Chem. Rev.* **2022**, *122*, 3459–3636.
[11] D. Wu, A. C. Sedgwick, T. Gunnlaugsson, E. U. Akkaya, J. Yoon, T. D. James, *Chem. Soc. Rev.* **2017**, *46*, 7105–7123.
[12] C. Guo, A. C. Sedgwick, T. Hirao, J. L. Sessler, *Coord. Chem. Rev.* **2021**, *427*, 213560.
[13] G. Picci, M. C. Aragoni, M. Arca, C. Caltagirone, M. Formica, V. Fusi, L. Giorgi, F. Ingargiola, V. Lippolis, E. Macedi, L. Mancini, L. Mummolo, L. Prodi, *Org. Biomol. Chem.* **2023**, *21*, 2968–2975.
[14] S. Ghosh, A. Rana, S. Biswas, *Chem. Mater.* **2024**, *36*, 99–131.
[15] Q. Wang, Z. Li, D.-D. Tao, Q. Zhang, P. Zhang, D.-P. Guo, Y.-B. Jiang, *Chem. Commun.* **2016**, *52*, 12929–12939.
[16] T.-T. Huang, J.-F. Chen, J. Liu, T.-B. Wei, H. Yao, B. Shi, Q. Lin, *Chin. Chem. Lett.* **2024**, *35*, 109281.
[17] Y. Jia, W.-L. Guan, J. Liu, J.-P. Hu, B. Shi, H. Yao, Y.-M. Zhang, T.-B. Wei, Q. Lin, *Chin. Chem. Lett.* **2023**, *34*, 108082.
[18] Q. Su, J. Chen, X. Sun, J. Liu, X. Dai, T. Wei, H. Yao, Q. Lin, *Chin. J. Chem.* **2024**, DOI: 10.1002/cjoc.202400394.
[19] X. Wu, X. Chen, B. Song, Y. Huang, Z. Li, Z. Chen, T. D. James, Y. Jiang, *Chem. Eur. J.* **2014**, *20*, 11793–11799.
[20] Y.-J. Huang, W.-J. Ouyang, X. Wu, Z. Li, J. S. Fossey, T. D. James, Y.-B. Jiang, *J. Am. Chem. Soc.* **2013**, *135*, 1700–1703.
[21] Y. Wu, Q. Zhang, Y. Zhao, K. Zhuang, Y. Fan, S. Zhang, X. Zhang, K. Huang, Z. Yao, *ACS Sustainable Chem. Eng.* **2020**, *8*, 6517–6523.
[22] Q. Han, Q. Wang, A. Gao, X.-P. Chang, L. Zeng, X. Cao, *ACS Sustainable Chem. Eng.* **2023**, *11*, 2139–2150.
[23] P. Gopikrishna, N. Meher, P. K. Iyer, *ACS Appl. Mater. Interfaces* **2018**, *10*, 12081–12111.
[24] S. V. Bhosale, C. H. Jani, S. J. Langford, *Chem. Soc. Rev.* **2008**, *37*, 331–342.
[25] Y. Ikawa, H. Ogawa, H. Harada, H. Furuta, *Bioorg. Med. Chem. Lett.* **2008**, *18*, 6394–6397.
[26] Y. Ohsedo, M. Oono, K. Saruhashi, H. Watanabe, *RSC Adv.* **2014**, *4*, 48554–48558.
[27] R. R. Kashapov, Y. S. Razuvayeva, A. Y. Ziganshina, R. K. Mukhitova, A. S. Sapunova, A. D. Voloshina, V. V. Syakaev, S. K. Latypov, I. R. Nizameev, M. K. Kadirov, L. Y. Zakharova, *Molecules* **2019**, *24*, 1939.
[28] C. Sosa-Gil, P. Cintas, J. C. Palacios, *Carbohydr. Res.* **2021**, *502*, 108278.
[29] H. Mesallati, N. A. Mugheirbi, L. Tajber, *Cryst. Growth Des.* **2016**, *16*, 6574–6585.
[30] P. I. Nagy, K. Takács-Novák, *J. Am. Chem. Soc.* **1997**, *119*, 4999–5006.
[31] N. C. Tansil, H. Xie, F. Xie, Z. Gao, *Anal. Chem.* **2005**, *77*, 126–134.
[32] P. Hao, Y. Xu, J. Shen, Y. Fu, *Dyes Pigm.* **2021**, *186*, 108941.
[33] F. Billeci, F. D'Anna, S. Marullo, R. Noto, *RSC Adv.* **2016**, *6*, 59502–59512.
[34] N. B. Kolhe, R. N. Devi, S. P. Senanayak, B. Jancy, K. S. Narayan, S. K. Asha, *J. Mater. Chem.* **2012**, *22*, 15235.
[35] P. Rajdev, M. R. Molla, S. Ghosh, *Langmuir* **2014**, *30*, 1969–1976.
[36] A. Pan, S. S. Mati, B. Naskar, S. C. Bhattacharya, S. P. Moulik, *J. Phys. Chem. B* **2013**, *117*, 7578–7592.
[37] M. Mahdiani, S. Rouhani, P. Zahedi, *J. Fluoresc.* **2023**, *33*, 2003–2014.
[38] R. Greiner, T. Schlücker, D. Zgela, H. Langhals, *J. Mater. Chem. C.* **2016**, *4*, 11244–11252.

[39] A. K. Srivastava, A. Singh, L. Mishra, *J. Phys. Chem. A* **2016**, *120*, 4490–4504.
[40] C. Rizzo, P. Cancemi, L. Mattiello, S. Marullo, F. D'Anna, *ACS Appl. Mater. Interfaces* **2020**, *12*, 48442–48457.
[41] S. Misra, P. Singh, A. Das, P. Brandão, P. Sahoo, N. Sepay, G. Bhattacharjee, P. Datta, A. K. Mahapatra, B. Satpati, J. Nanda, *Mater. Adv.* **2020**, *1*, 3532–3538.
[42] B.-P. Jiang, D.-S. Guo, Y. Liu, *J. Org. Chem.* **2010**, *75*, 7258–7264.
[43] F. Würthner, T. E. Kaiser, C. R. Saha-Möller, *Angew. Chem. Int. Ed.* **2011**, *50*, 3376–3410.
[44] H. Shao, T. Nguyen, N. C. Romano, D. A. Modarelli, J. R. Parquette, *J. Am. Chem. Soc.* **2009**, *131*, 16374–16376.
[45] H. Shao, M. Gao, S. H. Kim, C. P. Jaroniec, J. R. Parquette, *Chem. Eur. J.* **2011**, *17*, 12882–12885.
[46] S. Marullo, M. Feroci, R. Noto, F. D'Anna, *Dyes Pigm.* **2017**, *146*, 54–65.
[47] B. Heyne, *Photochem. Photobiol. Sci.* **2016**, *15*, 1103–1114.
[48] Z. Chen, A. Lohr, C. R. Saha-Möller, F. Würthner, *Chem. Soc. Rev.* **2009**, *38*, 564–584.
[49] P. J. Collings, E. J. Gibbs, T. E. Starr, O. Vafek, C. Yee, L. A. Pomerance, R. F. Pasternack, *J. Phys. Chem. B* **1999**, *103*, 8474–8481.
[50] J. C. de Paula, J. H. Robblee, R. F. Pasternack, *Biophys. J.* **1995**, *68*, 335–341.
[51] F. D'Anna, F. Ferrante, R. Noto, *Chem. Eur. J.* **2009**, *15*, 13059–13068.
[52] F. D'Anna, S. Marullo, P. Vitale, R. Noto, *Eur. J. Org. Chem.* **2011**, *2011*, 5681–5689.
[53] C. Rizzo, R. Arrigo, N. T. Dintcheva, G. Gallo, F. Giannici, R. Noto, A. Sutera, P. Vitale, F. D'Anna, *Chem. Eur. J.* **2017**, *23*, 16297–16311.
[54] F. D'Anna, P. Vitale, F. Ferrante, S. Marullo, R. Noto, *Chempluschem* **2013**, *78*, 331–342.
[55] B. Michen, C. Geers, D. Vanhecke, C. Endes, B. Rothen-Rutishauser, S. Balog, A. Petri-Fink, *Sci. Rep.* **2015**, *5*, 9793.
[56] S. Basak, N. Nandi, S. Paul, A. Banerjee, *ACS Omega* **2018**, *3*, 2174–2182.
[57] W. Z. Yuan, P. Lu, S. Chen, J. W. Y. Lam, Z. Wang, Y. Liu, H. S. Kwok, Y. Ma, B. Z. Tang, *Adv. Mater.* **2010**, *22*, 2159–2163.
[58] Q. Wu, T. Zhang, Q. Peng, D. Wang, Z. Shuai, *Phys. Chem. Chem. Phys.* **2014**, *16*, 5545–5552.
[59] Y. Ma, Y. Song, Y. Ma, F. Wei, G. Xu, Y. Cen, M. Shi, X. Xu, Q. Hu, *New J. Chem.* **2018**, *42*, 8992–8997.
[60] Y. Li, M. Sun, Y. Yang, H. Meng, Q. Wang, C. Li, G. Li, *J. Mater. Chem. C* **2021**, *9*, 8683–8693.
[61] F. Goudarzy, J. Zolgharnein, J. B. Ghasemi, *Inorg. Chem. Commun.* **2022**, *141*, 109512.
[62] Y. Mazouzi, A. Miche, A. Loiseau, B. Beito, C. Méthivier, D. Knopp, M. Salmain, S. Boujday, *ACS Sens.* **2021**, *6*, 3485–3493.
[63] S. Nazerdeylami, J. B. Ghasemi, G. Mohammadi Ziarani, A. Amiri, A. Badiei, *J. Mol. Liq.* **2021**, *336*, 116104.
[64] N. Wang, A. Majid, K. Wang, L. Tan, H. Li, J. Wang, *Mater. Sci. Semicond. Process.* **2023**, *167*, 107800.
[65] Z. Lu, G. Li, Y. Hu, *New J. Chem.* **2022**, *46*, 19153–19160.
[66] B. Mao, F. Qu, S. Zhu, J. You, *Sens. Actuators B* **2016**, *234*, 338–344.
[67] S. Rajendran, V. Usha Vipinachandran, K. H. Badagoppam Haroon, I. Ashokan, S. K. Bhunia, *Anal. Methods* **2022**, *14*, 4263–4291.
[68] J. N. Miller, *Analyst* **1991**, *116*, 3–14.

Manuscript received: May 19, 2024
Accepted manuscript online: August 16, 2024
Version of record online: ■■, ■■

RESEARCH ARTICLE

We employed two self-assembling fluorophores functionalized with D-Glucamine, as fluorescent sensors for emerging pollutants in water, such as drugs, belonging to different classes and differing significantly in structure.

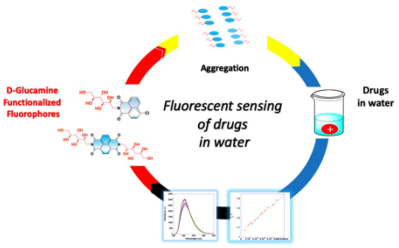

S. Marullo, R. Arena, G. Lazzara, G. Cavallaro, M. Cacioppo, F. D'Anna**

1 – 15

Fast and Efficient Sensing of Drugs in Water Using Self-Assembling D-Glucamine-Functionalized Naphthalenediimide and 1,8-Naphthalimide Fluorophores